RSC Advances

PAPER

View Article Online
View Journal | View Issue

Cite this: *RSC Adv.*, 2019, **9**, 15158

Insulating 3D-printed templates are turned into metallic electrodes: application as electrodes for glycerol electrooxidation†

Katia-Emiko Guima,[a] Victor H. R. Souza[b] and Cauê Alves Martins *[ab]

Received 25th February 2019
Accepted 1st May 2019

DOI: 10.1039/c9ra01436e

rsc.li/rsc-advances

We turned printed plastic pieces into a conductive material by electrochemical polymerization of aniline on the plastic surface assisted by graphite. The conductive piece was then turned into a metallic electrode by potentiodynamic electrodeposition. As a proof-of-concept, we built indirect-3D-printed Pd, Pt and Au electrodes, which were used for glycerol electrooxidation.

Additive manufacturing, or 3D-printing, is a revolutionary technique which allows for the easy fabrication of three-dimensional objects, enabling the construction of complex devices with minimum waste and very low cost, which previously could only have been fabricated with sophisticated equipment and facilities.[1,2] This technology has attracted attention from industry and academia due to the myriad architectures, materials and applications.[2–4] Among the various 3D-printing methods, extrusion through fused deposition modeling (FDM) is the most commonly used. This method, in which a thermoplastic is forced through a heated nozzle head, was invented in 1989 by Scott Crump,[5] and is currently the most affordable and commercialized way of 3D-printing.

The field of electrochemistry has benefited from 3D-printing technologies. Ambrosi and Pumera have detailed the advances brought by additive manufacturing to electrochemistry, including instruments, sensors and materials.[2] In particular, the ability to rapidly prototype new parts and devices boosted the advancement in instrumentation used for electrochemistry.[2,6,7]

Our group printed a three-parts electrolyzer with an approximate cost of US $5.[8] This device was used with Pd-nanocubes-modified glassy carbon as working electrode to convert glycerol into tartronate.[8] Concerning microfluidics, 3D-printing is already considered a revolution in microfluidics, due to the ability of partially or completely replacing poly(dimethylsiloxane) pieces built by soft lithography.[9]

FDM technique has recently opened up the possibility of printing conductors, which can be used as electrodes for a variety of applications. The biggest challenge is to print ready-to-use electrodes, since the extrusion of composite thermoplastic/metal is still rare. In this sense, much effort has been spent to build and print plastic/carbon materials[10–12] and to modify existing printed objects.[4,11] Wei *et al.* produced graphene oxide (GO) blended with acrylonitrile butadiene styrene (ABS) or polylactic acid (PLA) to build a GO-thermoplastic filament for the first time.[10] The authors also reduced GO to rGO with hydrazine hydrate in order to make a rGO-thermoplastic filament.[10] Another remarkable achievement was made by Rymansaib *et al.*[12] These authors made a new filament of polystyrene/carbon-nanofiber/graphite simultaneously printed embedded in an insulating material, composing a monolithic object, which is electrochemically stable and prospective for electroanalysis.[12]

Palenzuela *et al.* developed a simple protocol to achieve the theoretical electrical conductivity predicted for printed graphene/PLA electrodes.[11] They exposed the printed electrodes to dimethylformamide in order to dissolve the fused polymer on the electrode surface. This procedure allows the authors to access the active sites of the electrode, which is used for electroanalysis.[11] Aside from thermoplastic/carbon materials, there is an impending need to build metallic 3D-printed electrodes. A successful post-printed modification was made by Díaz-Marta *et al.* to produce Pd- and Cu-based materials for heterogeneous organic synthesis.[4] By following complex steps, the authors printed a SiO_2 material, which was chemically treated in sequential steps to be finally modified with CuI and $Pd(AcO)_2$ to produce Cu and Pd catalysts.[4] The development of metal-based 3D-printed materials for a wide range of electrochemistry applications using simple protocols is still necessary.

Here, we used FDM to print PLA templates, which are modified with precursors of a conducting polymer and graphite (GR). This material is submitted to electrochemical polymerization, allowing further metallic electrodeposition. As proof-of-concept, we prepared Pd, Pt and Au electrodes built on 3D-printed templates. These electrodes were then used for glycerol electrooxidation to investigate their applicability as anodes of glycerol fuel cells and electrolyzers.[13–15]

[a]*Faculty of Exact Sciences and Technology, Federal University of Grande Dourados, Rodovia Dourados - Itahum, km 12, 79804-970, Dourados, MS, Brazil*

[b]*Physics Institute, Federal University of Mato Grosso do Sul, Av. Costa e Silva, 79070900, Campo Grande, MS, Brazil. E-mail: caue.martins@ufms.br*

† Electronic supplementary information (ESI) available. See DOI: 10.1039/c9ra01436e

We used. PLA as the thermoplastic filament in a commercially available 3D-printer (Sethi 3D, model S3). A CAD model of the electrode was drawn using software Autodesk Inventor 2017 and further sliced using software Simplify 3D. The electrodes are chosen to have dimensions of $3 \times 3 \times 5$ mm^3 so that they could be connected to a regular alligator connector, as shown in Fig. 1. The template is modified in aniline and HCl solution and further modified with graphite 99.69% (ashes 0.31%; humidity 0.06%; 13.33% retained in 100# grid and 97.40% in 325# grid). The procedures for such modifications are detailed through the text.

The printing parameters of the working electrode template are summarized in Table S1.† The total building time is only 1 min and material cost is 0.01 US $, which is a very low price and a fast way of obtaining the templates. It is worth noting that the printing parameters found in Table S1† change whether one changes the size and shape of the desired template.

The post-printing treatment developed here is based on a surface polymerization reaction for growing polyaniline (PAni) on PLA. The 3D-printed template is immersed in a mixture of 1 mL aniline with 2 mL 1 mol L^{-1} HCl in order to place the polymer precursor, aniline chloride ($C_6H_5NH_3^+Cl^-$) on the PLA surface. The aim is to polymerize the precursor on the template to become conducting. The electrochemical synthesis of PAni has been previously described.[16,17] This conducting polymer is structurally different depending on the oxidation state. The reduced form, which has a yellow color, is leucoemeraldine. This form can be electrooxidized to emeraldine, which is blue in an alkaline medium or green in an acidic medium, as shown in Fig. S1.† Emeraldine can be further oxidized to pernigraniline (violet color). In order to maintain structural stability during the electrochemical measurements, the reduced form leucoemeraldine/emeraldine is desirable, while further oxidation of emeraldine may accelerate degradation. This process has been widely discussed in the literature, as those for metal polymerization *via* electrochemistry.[18,19] For these previous studies, the substrate of the polymerization was already a conducting material, facilitating the electric contact with the voltage source (*e.g.* potentiostat/galvanostat), represented by an "aligator" in Fig. 1. However, in the present case, the challenge is that the widely used 3D-printed PLA is an insulating material.

To surpass this issue, we developed GR-assisted polymerization. Immersing the template in the aniline chlorite solution smoothly melts the PLA surface. The template is then transferred to a glass container with GR and gently shaken until the PLA is completely covered. The GR-modified printed piece is finally dried at room temperature for 20 h. After dried, the template is washed with D.I. water under stirring for 10 min. This process is repeated five times and it is imperative to spread out unattached GR. Finally, the electrode is transferred to an electrochemical cell for the electrochemical polymerization of aniline in 1 mol L^{-1} HCl. Once impossible electrochemical polymerization of aniline over PLA, is now achievable by cyclic voltammetry. The electrolyte accesses the template surface covered with $C_6H_5NH_3^+Cl^-$ as it goes through the GR flakes, while GR makes the connection between the electric connector (alligator connected to the potential source) and the electrolyte, allowing for electrochemical polymerization, as illustrated in Fig. 1.

The GR-assisted electrochemical polymerization of the GR/$C_6H_5NH_3^+Cl^-$/PLA template is shown in Fig. 2. The growth of PAni is evidenced through the increase of two redox coupled peaks at low (I/I′) and high (II/II′) potentials. The oxidation of leucoemeraldine to emeraldine starts at 0.35 V, displaying an evident peak centered at 0.48 V (peak I in Fig. 2). Emeraldine is further oxidized to pernigraniline, displaying a peak at 0.73 V (peak II in Fig. 2). During the negative potential scan, pernigraniline is reduced to emeraldine at ~0.7 V and further reduced to leucoemeraldine with a cathodic transient centered at 0.25 V, as shown by peaks II′ and I′ respectively in Fig. 2. The potential cycles were performed until the redox couple I/I′ is evident, which takes place after ~30 cycles. At this point, the PLA is mainly covered by emeraldine, making it a conducting electrode.

The electrode resistance of the polymerized material is 45 Ω, which is acquired by measuring the high frequency intercept of the Nyquist plot in an electrochemical impedance spectroscopy analysis performed at 106 Hz. The electrochemical profile shown in Fig. 2 associated to the low resistance demonstrates the success of the GR-assisted polymerization. Furthermore, the resistance measured with a multimeter is ~36 Ω cm^{-1}, which reveals

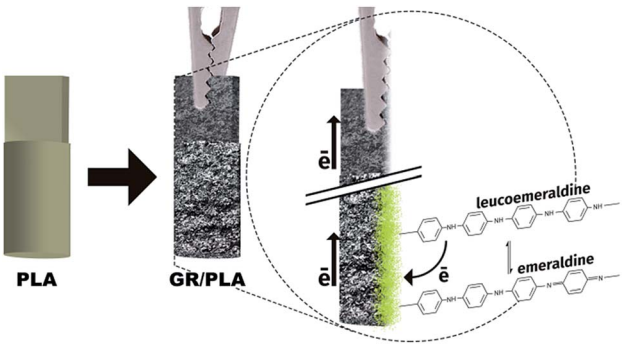

Fig. 1 Illustrative scheme of the graphite-assisted electrochemical polymerization of polylactic acid template electrodes. The PLA template is covered by aniline precursor and graphite, which is further electrochemically polymerized to emeraldine (and other PANI structures in different oxidation states).

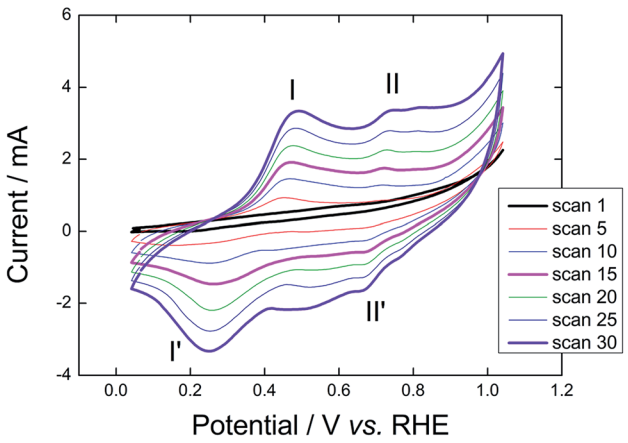

Fig. 2 Graphite-assisted electrochemical polymerization of GR/$C_6H_5NH_3^+Cl^-$/PLA template in 1 mol L^{-1} HCl at 0.05 V s^{-1}.

a remarkable conducting material. GR has a double contribution on the electrode construction; one is assisting polymerization, working as an electron collector (previously discussed) while also contributing to the increase in conductivity after polymerization. It is worth noting that GR used with other organochlorides does not show similar performance. As an example, we smoothly melted the PLA template in dichloromethane and dispersed GR on it. In such case, the resulting composite showed high resistance, in the MΩ scale. Therefore, PAni coverage is imperative to the increase in electrical conductivity of the template.

After turning the PLA into an electrical conductor to form a GR/PAni/PLA template, the printed piece was immersed in a 6 mmol L^{-1} $PdCl_2$ in 0.5 mol L^{-1} H_2SO_4 for Pd electrodeposition. The metallic deposition was achieved by applying successive potential cycles between 0.019 and 1.319 V. Potentiodynamic deposition allows us to observe the formation of a Pd electrode through the appearance of a Pd profile, *i.e.* we can *in situ* evaluate the growth of Pd on the template. In other words, once a characteristic profile of Pd in acidic media is identified, we are certain of a success deposition. The experimental details of the electrochemical measurements are found in the ESI Section II.†

Fig. 3A shows an increase in anodic and cathodic currents wherein successive potential cycles are applied. Pd^{2+} is reduced to Pd on the template during the cycles and the currents related to the Pd surface reaction in aqueous acid solution become more evident. After identifying an obvious profile of Pd, the electrode was transferred to an electrochemical cell containing 0.1 mol L^{-1} KOH in order to measure a profile in a controlled system.

Fig. 3B undoubtedly evidences a characteristic profile of Pd through the cyclic voltammogram in the range of 0.15–1.27 V. Surface oxide formation starts at ~0.7 V during the positive potential sweep, which is reduced producing a cathodic current, forming a peak centered at ~0.7 V. Another pivotal characteristic is the hydrogen under potential deposition (H_{UPD}) region at around 0.15–0.5 V. Overall, this electrochemical profile shows that a Pd electrode was indeed manufactured.[20]

The indirect-3D-printed Pd electrode was then used as a working electrode in the presence of 0.2 mol L^{-1} glycerol in 0.1 mol L^{-1} KOH, as shown in Fig. 3C. The cyclic voltammograms display anodic currents during the positive and negative potential sweeps. The current density increases with successive cycles due to the initial cleaning of the surface, until a stable profile is reached at the fifth cycle. Such a phenomenon was previously reported for Pd catalyst.[21] During the positive scan, electrooxidation starts at ~0.6 V, reaching a maximum at ~1.08 V. During the reverse scan, the surface reactivation after the reduction of Pd surface oxides promotes an accentuated oxidation peak centered at 0.76 V; these potentials match the electrocatalytic parameters reported for commercial Pd/C.[13]

The Pd electrode was also investigated by EDS mapping of the Pd electrode in order to qualitative characterize the chemical composition (experimental details in ESI Section III†). Firstly, the morphology of the electrode investigated *via* SEM reveals nanostructures built onto the GR (Fig. 3D). The Pd particles do not have well-defined shapes and are slightly agglomerated. The size of the particles ranges between approximately 100–450 nm. A section of an SEM image (Fig. 3E) was then used to qualitatively investigate

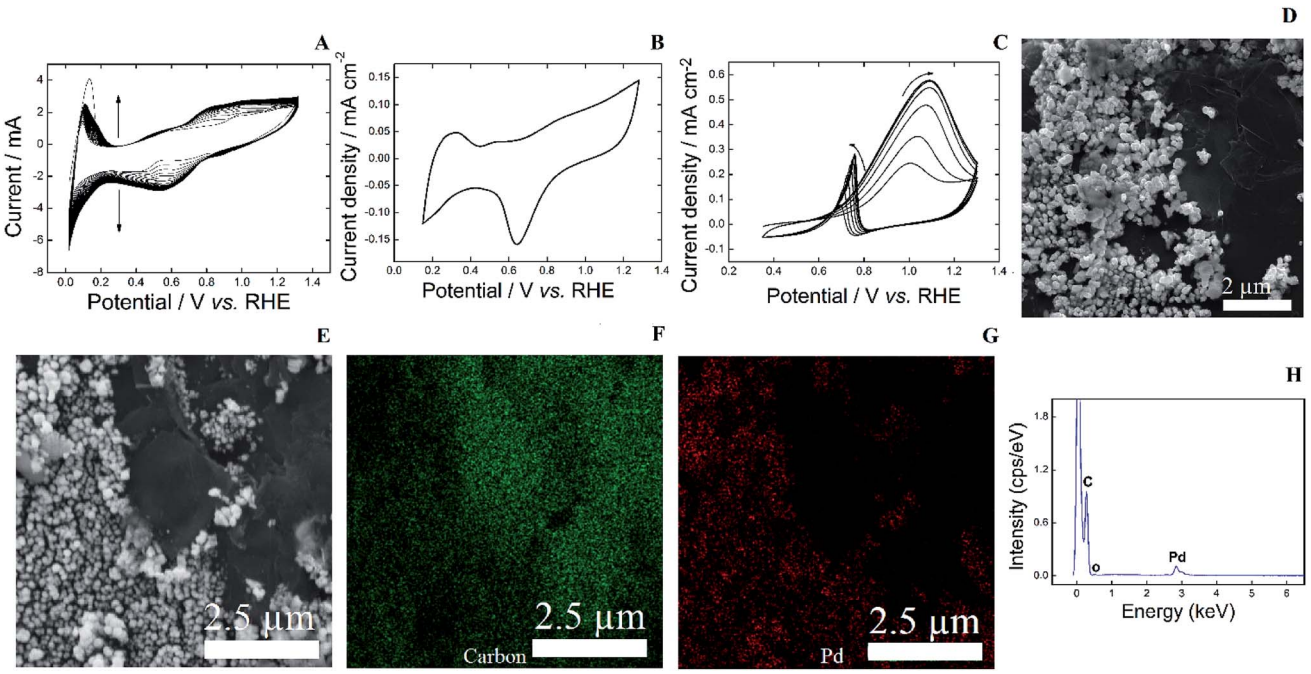

Fig. 3 (A) Potentiodynamic electrodeposition process achieved by successive potential cycles of GR/PAni/PLA template in 6 mmol L^{-1} $PdCl_2$ in 0.5 mol L^{-1} H_2SO_4, measured between 0.019 and 1.31 V. (B) Cyclic voltammogram of the indirect-3D-printed Pd electrode in 0.1 mol L^{-1} KOH, measured between 0.15 and 1.27 V and (C) in the presence of 0.2 mol L^{-1} glycerol between 0.35 and 1.29 V. All measurements are performed at 0.05 V s^{-1}. (D) and (E) show representative SEM images, while (F) and (G) show EDS Kα elemental composition maps (indicated in the figure). (H) EDS spectrum of the indirect-3D-printed Pd electrode.

the chemical composition of a Pd electrode using EDS. Fig. 3F shows an image highlighting the presence of carbon on the electrode surface, whereas Fig. 3G highlights the presence of Pd. The large region with high presence of Pd (Fig. 3G) overlaps with the region of Pd particles from the SEM image (Fig. 3E). Moreover, the wide carbon region (Fig. 3E) is indicated by the high-intensity green colored region on the EDS mapping (Fig. 3F). These findings assure the presence of the metal and carbon on the printed template. Finally, an EDS spectrum shows the presence of Pd through a peak at ~2.84 keV (Fig. 3H). Aiming the manufacturing of noble metal-based indirect-3D-printed, we built Pt and Au electrodes, which were both applied for glycerol electrooxidation, as described in ESI Section IV.†

In summary, we successfully turned an insulating 3D-printed piece into a mostly metallic piece with low resistivity. The present research shows a low-cost alternative to build metallic electrodes or metallic pieces suitable for different sizes and shapes of a 3D-printed template with multipurpose. This sustainable protocol allows for the modification of any existing printed material, so it is an alternative for recycle and/or reuse of existing materials, showing that low-cost and widely available thermoplastic filaments of FDM 3D-printers can be used as source of template. This work opens up the possibility of indirect-3D-printing any metallic piece in any shape.

Conclusions

A simple protocol was developed to surpass the challenge of obtaining conductive 3D-printed pieces by fused deposition modeling. A plastic filament was used to print small pieces further electrochemically covered with polyaniline, which is achieved by using graphite to connect the source of voltage and the electrolyte. This conductive piece is then turned into metallic electrode by electrodeposition. This protocol can be used to recycle an existing plastic piece turning it into a metallic one in a sustainable way.

As a proof-of-concept, we built Pd, Pt and Au pieces, which were used as electrodes for glycerol electrooxidation. The electrochemical profiles, in the absence and presence of glycerol, in addition to microscopy images demonstrate that metallic pieces can be successfully manufactured. The indirect-3D-printed metallic electrodes were used for an alcohol electrooxidation in order to suggest their use in electrocatalysis; however, the electrodes built here may be used for analytical purposes, as sensors.

Furthermore, we firstly report a simple electrochemical way of turning a printed insulator into a metallic piece. Therefore, the applications go beyond the electrochemistry field, since metallic pieces may be manufactured following a simple model in a shape and size previously forecasted by the researcher or industrialist. This method may be applied to build electronic compartments, in a morphology previously predicted simply by modelling instead of machining it.

Conflicts of interest

There are no conflicts to declare.

Acknowledgements

The authors acknowledge CNPq (Grant #454516/2014-2), FUNDECT (Grants #026/2015 and #099/2016), CAPES and FINEP. The authors also thank Dr A. J. G. Zarbin for the SEM images.

Notes and references

1 C. Parra-Cabrera, C. Achille, S. Kuhn and R. Ameloot, *Chem. Soc. Rev.*, 2018, **47**, 209–230.
2 A. Ambrosi and M. Pumera, *Chem. Soc. Rev.*, 2016, **45**, 2740–2755.
3 M. Hofmann, *ACS Macro Lett.*, 2014, **3**, 382–386.
4 A. S. Díaz-Marta, C. R. Tubío, C. Carbajales, C. Fernández, L. Escalante, E. Sotelo, F. Guitián, V. L. Barrio, A. Gil and A. Coelho, *ACS Catal.*, 2017, 392–404.
5 S. S. Crump, *US Pat.*, 5121329 A, 1992.
6 G. W. Bishop, J. E. Satterwhite, S. Bhakta, K. Kadimisetty, K. M. Gillette, E. Chen and J. F. Rusling, *Anal. Chem.*, 2015, **87**, 5437–5443.
7 S. Waheed, J. M. Cabot, N. P. Macdonald, T. Lewis, R. M. Guijt, B. Paull and M. C. Breadmore, *Lab Chip*, 2016, **16**, 1993–2013.
8 K.-E. Guima, L. M. Alencar, G. C. da Silva, M. A. G. Trindade and C. A. Martins, *ACS Sustainable Chem. Eng.*, 2018, **6**, 1202–1207.
9 N. Bhattacharjee, A. Urrios, S. Kang and A. Folch, *Lab Chip*, 2016, **16**, 1720–1742.
10 X. Wei, D. Li, W. Jiang, Z. Gu, X. Wang, Z. Zhang and Z. Sun, *Sci. Rep.*, 2015, **5**, 11181.
11 C. L. Manzanares Palenzuela, F. Novotný, P. Krupička, Z. Sofer and M. Pumera, *Anal. Chem.*, 2018, **90**(9), 5753–5757.
12 Z. Rymansaib, P. Iravani, E. Emslie, M. Medvidović-Kosanović, M. Sak-Bosnar, R. Verdejo and F. Marken, *Electroanalysis*, 2016, **28**, 1517–1523.
13 T. S. D. Almeida, K.-E. Guima, R. M. Silveira, G. C. da Silva, M. A. U. Martines and C. A. Martins, *RSC Adv.*, 2017, **7**, 12006–12016.
14 G. L. Caneppele, T. S. Almeida, C. R. Zanata, É. Teixeira-Neto, P. S. Fernández, G. A. Camara and C. A. Martins, *Appl. Catal., B*, 2017, **200**, 114–120.
15 C. R. Zanata, P. S. Fernández, H. E. Troiani, A. L. Soldati, R. Landers, G. A. Camara, A. E. Carvalho and C. A. Martins, *Appl. Catal., B*, 2016, **181**, 445–455.
16 L. J. Duić, Z. Mandić and F. Kovačiček, *J. Polym. Sci., Part A: Polym. Chem.*, 1994, **32**, 105–111.
17 Y.-B. Shim, M.-S. Won and S.-M. Park, *J. Electrochem. Soc.*, 1990, **137**, 538–544.
18 A. Nirmala Grace and K. Pandian, *Electrochem. Commun.*, 2006, **8**, 1340–1348.
19 A. Eftekhari, L. Li and Y. Yang, *J. Power Sources*, 2017, **347**, 86–107.
20 A. E. Bolzán, *J. Electroanal. Chem.*, 1995, **380**, 127–138.
21 C. A. Martins, P. S. Fernández, H. E. Troiani, M. E. Martins, A. Arenillas and G. A. Camara, *Electrocatalysis*, 2014, **5**, 204–212.